

# N-terminal RAG1 frameshift mutations in Omenn's syndrome: Internal methionine usage leads to partial V(D)J recombination activity and reveals a fundamental role *in vivo* for the N-terminal domains

Sandro Santagata\*, Carlos A. Gomez\*, Cristina Sobacchi<sup>†</sup>, Fabio Bozzi<sup>†</sup>, Mario Abinun<sup>‡</sup>, Srdjan Pasic<sup>§</sup>, Patricia Cortes<sup>¶</sup>, Paolo Vezzoni<sup>¶</sup>, and Anna Villa<sup>†</sup>

\*Ruttenberg Cancer Center, <sup>¶</sup>Immunobiology Center, Mount Sinai School of Medicine, 1425 Madison Avenue, New York, NY 10029; <sup>†</sup>Department of Human Genome and Multifactorial Disease, Istituto di Tecnologie Biomediche Avanzate, Consiglio Nazionale delle Ricerche, via Fratelli Cervi 93, 20090 Segrate (MI), Italy; <sup>‡</sup>Children's Bone Marrow Transplant Unit, Newcastle General Hospital, Newcastle upon Tyne NE4 6BE, United Kingdom; and <sup>§</sup>Pediatric Immunology, Mother and Child Health Institute, Belgrade, Yugoslavia

Communicated by Renato Dulbecco, The Salk Institute for Biological Studies, San Diego, CA, October 23, 2000 (received for review May 2, 2000)

Omenn's syndrome is an autosomal recessive primary immunodeficiency characterized by variable numbers of T lymphocytes of limited clonality, hypereosinophilia, and high IgE levels with a paradoxical absence of circulating B lymphocytes. We have previously attributed this disorder to missense mutations that render the RAG1/RAG2 recombinase only partially active. Here we report seven Omenn's patients with a novel class of genetic lesions: frameshift mutations within the 5' coding region of RAG1. Interestingly, we demonstrate in transient expression experiments that these frameshift deletion alleles remain partially functional for both deletional and inversional recombination and can hence explain the partial rearrangement phenotype observed in these patients. The rearrangement activity is mediated by truncated RAG1 proteins that are generated by alternative ATG usage 3' to the frameshift deletion and that demonstrate improper cellular localization. Taken together, our results suggest a novel mechanism for the development of immunodeficiency in a subset of Omenn's syndrome patients.

The development of T and B lymphocytes is dependent on the coordinated action of a complex genetic network consisting of growth factors, cell signaling molecules, and transcription factors. Primary immunodeficiencies can result from mutations in components of this developmental program that block lymphocyte development (1). Mutations in the lymphoid-specific components RAG1 and RAG2 that are critical for the V(D)J recombination process can also lead to immunodeficient states. In humans, severe combined immunodeficiency with an absence of mature T and B cells can result from missense and nonsense mutations that abrogate the recombination efficiency of RAG1/RAG2 (2). In addition, less severe missense mutations in RAG1/RAG2 that render the recombinase only partially active can lead to Omenn's syndrome (3, 4). This clinically variable disease is characterized by early onset erythrodermia, hepatosplenomegaly, hypereosinophilia, high IgE levels, low to absent levels of B lymphocytes, and normal to low numbers of activated, anergic, oligoclonal T lymphocytes.

The RAG1/RAG2 recombinase directs the nucleolytic cleavage events that are required to mediate somatic assembly of the antigen receptor gene segments. This process involves recognition and synapsis of a pair of recombination signal sequences (RSS) containing spacers with conserved heptamer and nonamer motifs separated by a relatively nonconserved spacer of either 12 or 23 bp (5–8). RAG1/RAG2 then introduce a double-strand break at the border of the RSS and the coding flank (9, 10). RAG1/RAG2 can also process hairpin interme-

diates (11, 12) and 3' flap overhangs that are postulated recombination intermediates (13).

V(D)J recombination can be mediated by a truncated form of RAG2 (amino acids 1–371) that contains six predicted kelch repeat motifs (14) along with a truncated form of RAG1 (amino acids 384–1008) that includes the RAG1 nonamer binding domain (15, 16) and the active site composed of a triplet of acidic amino acids (17–19). Although it is dispensable for recombination, the N terminus of RAG1 (amino acids 1–383) has been conserved throughout vertebrate evolution and indeed enhances the efficiency of the rearrangement reaction. It appears that conserved cysteine elements (20) and a basic amino acid motif (21) in this region can enhance the recombination activity of RAG1. The N terminus also contains a dimerization domain defined by a C<sub>3</sub>HC<sub>4</sub> zinc binding motif and a C<sub>2</sub>H<sub>2</sub> zinc finger (22) as well as a nuclear localization signal important for interaction with the nuclear localization factor Srp1 (23, 24).

Here we report that a subset of individuals with Omenn's syndrome have one or two nucleotide deletions at the N terminus of RAG1 that predict frameshifts leading to the production of nonfunctional RAG1 fragments that lack large portions of the C terminus. Surprisingly, we demonstrate that amino-terminal truncated forms of RAG1 are generated from these alleles by initiation from internal methionines downstream of the frameshift lesions and that these alleles are competent for recombination. These findings suggest a novel mechanism for the etiology of immunodeficiency in humans.

## Materials and Methods

**Identification of Mutations in RAG1 and Generation of Recombinant Plasmid Constructs.** Patients were diagnosed as having OS according to the criteria previously detailed (3, 4). Mutations in RAG1 (GenBank M29474) were identified as previously described (3). Identified deletions Δ368A/369A and Δ887A were introduced into a eukaryotic expression vector [pEBB under the transcriptional control of the polypeptide elongation factor 1α promoter (25)] by PCR amplification of an approximately 410-bp fragment

Abbreviations: RAG, recombination activating gene; RSS, recombination signal sequence; OS, Omenn's syndrome; HA, hemagglutinin.

<sup>¶</sup>To whom reprint requests should be addressed. E-mail: vezzoni@itba.mi.cnr.it.

The publication costs of this article were defrayed in part by page charge payment. This article must therefore be hereby marked "advertisement" in accordance with 18 U.S.C. §1734 solely to indicate this fact.

from the start ATG to the *AvrII* site followed by multifragment ligations of the PCR products and an *AvrII*–*NotI* fragment from wild-type human Rag1 into pEBB opened *BamHI*–*NotI*. HA tags were introduced by PCR from the *Bsu36 I* site of RAG1 to the 3' *NotI* site with a 3' oligonucleotide encoding the nine amino acid hemagglutinin (HA) tag (YPYDVDPYA) followed by a TAA stop codon. Constructs containing RAG1 initiated from methionines 183, 202, 263, 324, and 355 were generated by PCR amplification, using a primer starting from the indicated methionine and another 3' of the *SphI* site. PCR products were subcloned into the *BamHI* and *SphI* sites of wild-type RAG1–3'HA. Fusions to the N terminus of green fluorescent protein were created by using pEGFPN3 (CLONTECH) by PCR amplification from the 3' end of RAG to the *Bsu36 I* site and cloned in frame with the *KpnI* of the vector. A *BamHI*–*Bsu36 I* fragment from wild-type and deletion mutant RAG1 proteins was used in the ligation with the *Bsu36 I*–*KpnI* PCR fragment between the *BglII*–*KpnI* sites of pEGFPN3. Sequences of PCR-amplified portions were verified by direct sequencing, by using the Thermosequense kit (United States Biochemical).

**Cellular Localization of Green Fluorescent Protein Fusions of RAG1 Proteins in 293T Cells.** Ten micrograms of pEGFPN3 constructs containing wild-type,  $\Delta 368A/369A$ , and  $\Delta 887A$  forms of RAG1 were transiently overexpressed in 293T cells by calcium phosphate transfection. Cells were processed as previously described (26). Images were acquired by confocal laser scanning microscopy.

**Nuclease and Electrophoretic Mobility Shift Assays.** 12 RSS cleavage assays and mobility shift assays were performed under 10% DMSO cleavage conditions previously described (27). Cleavage assays were incubated for 30 min at 37°C. Binding assays were performed at 30°C for 10 min in  $Mg^{2+}$  with the subsequent addition of 0.1% glutaraldehyde followed by an additional 10 min at 30°C.

**In Vivo Recombination Assays and Interaction Analysis.** Recombination conditions were modifications of those established by Hesse *et al.* (28) and recently described by Aidinis *et al.* (29), by using recombination substrates pJH200 and pJH288 (28) cotransfected with pEBG RAG expression constructs in 293T cells. Plasmid was isolated 48 h after transfection and used in a PCR-based method to evaluate the formation of signal and coding joints (3, 30). To ensure that PCR analysis provided a semiquantitative assessment of recombination activity, assays were performed within a dilution range where the intensity of the bands decreased proportionally to the dilution of the input DNA. Signal joints were detected by using PCR primers RA5 and RA14; coding joints, using primers OOP2 and CR3 or RA2 and CR3 (3, 30); and loading controls, with primers RA1C and RA6.

**Affinity Purification of <sup>35S</sup>-Labeled HA-RAG1 Proteins.** 293T cells were transfected with 10  $\mu$ g of RAG1(WT)-3'HA, RAG1( $\Delta 368A/369A$ )-3'HA, and RAG1( $\Delta 887A$ )-3'HA, and HA-tagged proteins were visualized after metabolic labeling and affinity purification as described (31).

**Affinity Purification of *gstRAG2/RAG1*-3'HA Proteins and Western Blot Analysis.** 293T cells were cotransfected with pEBGRAG2 (amino acids 1–383) and pEBB-RAG1(WT)-3'HA, RAG1( $\Delta 887A$ )-3'HA, RAG1(methionine 324)-3'HA, or RAG1(methionine 355)-3'HA. Interactions were analyzed as described (3). Complexes were isolated on glutathione beads, resolved by SDS/PAGE, transferred to nitrocellulose, blotted with anti-HA antibody 12CA5, and visualized with an anti-

**Table 1. Nucleotide mutations and corresponding alterations in the protein sequence for seven Omenn's patients**

Patient	Nucleotide	Amino acid (aa) changes
OS5	1. Deletion 368–369	Frameshift at P85 + 32 aa added before STOP
	2. A1398G	D429G
OS8	1. Deletion 368–369	Frameshift at P85 + 32 aa added before STOP
	2. Deletion 368–369	Frameshift at P85 + 32 aa added before STOP
OS9	1. Deletion 368–369	Frameshift at P85 + 32 aa added before STOP
	2. C1982T	R624C
OS10	1. Deletion 368–369	Frameshift at P85 + 32 aa added before STOP
	2. G2667A	E722K
OS11	1. Deletion 368–369	Frameshift at P85 + 32 aa added before STOP
	2. G2599T, A2600T	R829X, STOP
OS12	1. Deletion 368–369	Frameshift at P85 + 32 aa added before STOP
	2. 19nt duplication of 2020 to 2038	Frameshift
OS13	1. Deletion 887	Frameshift at S258 + 4 aa added before STOP
	2. Deletion 887	Frameshift at S258 + 4 aa added before STOP

OS5 has previously been described (3).

mouse secondary antibody conjugated to horseradish peroxidase with ECL (Amersham Pharmacia).

## Results

We have previously identified missense mutations in both RAG genes as a cause of Omenn's syndrome (3). To further characterize the molecular basis of this disorder, we analyzed the RAG1/RAG2 genetic locus of a large group of newly identified Omenn's patients. Through this extensive analysis we detected seven patients who manifested the characteristics of Omenn's syndrome and who have similar deletions at the N terminus of RAG1 (Table 1). OS8 was homozygous for a two-nucleotide deletion ( $\Delta 368A/369A$ ) toward the 5' end of the RAG1 ORF. OS5 and OS9–12 were compound heterozygous for the same frameshift deletion and another mutated allele that varied between individuals.  $\Delta 368A/369A$  leads to a frameshift at proline 85 and predicts the addition of 32 aberrant amino acids before a premature stop codon is encountered. Another patient OS13 was homozygous for a single nucleotide deletion  $\Delta 887A$ . Deletion of 887A creates a frameshift at serine 258 with the addition of four amino acids before a stop codon is found. In all cases, the frameshifted alleles predict the generation of severely truncated, recombinationally inactive proteins of either 117 or 262 amino acids.

Because two of the patients (OS8 and OS13) were homozygous for frameshifted alleles and another two (OS11 and OS12) had the frameshifted alleles coupled to forms of RAG1 that were likely inactive, the possibility arose that the alleles bearing the deletions could provide the partial recombination activity needed to generate a T cell repertoire of limited clonality. To investigate this possibility, we transfected 293T cells with the plasmid pEBB expressing full-length untagged RAG1 genes containing either the wild-type sequence or a deletion of either 368A/369A or 887A. The cells were cotransfected with the pEBG plasmid expressing *gstRAG2* (amino acids 1–371) along with either the pJH200 (deletional) or the pJH288 (inversional)

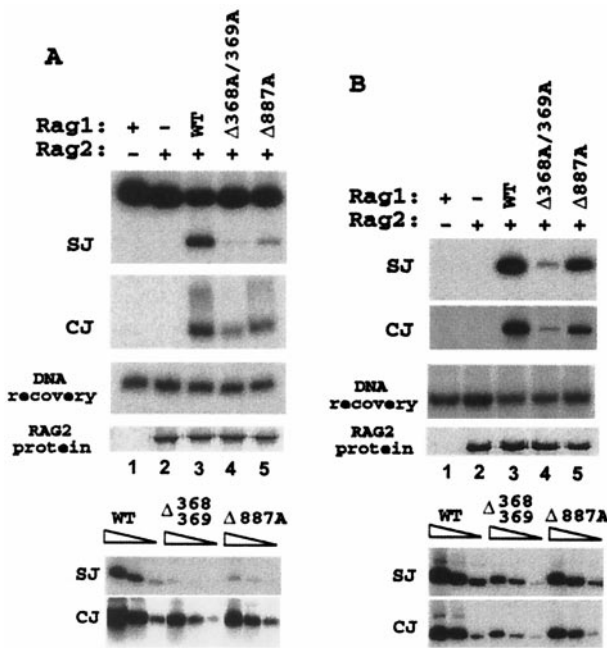


**Fig. 1.** RAG1 alleles with frameshift deletions of 368A/369A and 887A in RAG1 are active for recombination of episomal plasmid substrates. Full-length wild-type (WT) and mutant alleles ( $\Delta 368A/369A$  and  $\Delta 887A$ ) were cotransfected into 293T cells with pEBG2 $\Delta C$  along with the deletion substrate pJH200 (A) and the inversion substrate pJH288 (B). Harvested plasmids were analyzed for signal joint (SJ) and coding joint (CJ) formation by PCR within the linear range of the assays as determined by serial dilutions (1:10, 1:40, 1:100) of the harvested plasmid (Lower). The PCR reaction products displayed in the upper panel were generated with the recovered DNA diluted at 1:50. PCR loading controls within the linear range are also displayed (DNA recovery), along with a Western blot using anti-gst antibody to detect levels of gstRAG2 protein in each assay.

recombination substrates. Analysis of both signal joint and coding joint recombination products by PCR (Fig. 1) revealed that the  $\Delta 368A/369A$  and  $\Delta 887A$  alleles were able to foster both deletional (Fig. 1A) and inversional (Fig. 1B) recombination, albeit at lower levels as compared with wild-type RAG1. Hence we conclude that RAG1 alleles with frameshifts toward the 5' end maintain the capacity to mediate V(D)J recombination.

We next evaluated whether the alleles producing mutated RAG1 proteins D429G, R624C, E722K, and R829X that were coupled to the frameshift alleles (in patients OS5, OS9, OS10, and OS11) could provide the recombination activity leading to the development of a partial antigen receptor repertoire. We assayed these mutations for 12 RSS binding (Fig. 2A) and cleavage (Fig. 2B) and for recombination by using the deletion substrate pJH200 (Fig. 2C). Because the proteins were severely inhibited in all assays, it appears that the partial recombination phenotype observed in the compound heterozygote patients resulted from the activity of the frameshift deletion alleles and not from the alleles to which they were coupled.

The ability of RAG1 alleles with deletions to allow recombination suggested three models. First the deletions may alter the RNA structure so as to trigger a ribosomal shifting (32) that would place the ribosome in the proper reading frame to generate an essentially full-length form of the RAG1 protein. Second, translational bypassing could occur at the sites of deletion where the translational machinery passes across a gap in the coding sequence of an RNA, yet still produces a single in-frame polypeptide (33). Third, initiation of truncated forms of RAG1 could occur from methionines downstream of the frameshift deletion. To test these possibilities we undertook a series of analyses.

To determine whether RAG1 protein could be produced from the  $\Delta 368A/369A$  and  $\Delta 887A$  alleles we generated fusion constructs of green fluorescent protein to the C terminus of the wild-type and frameshift forms of RAG1 and attempted to

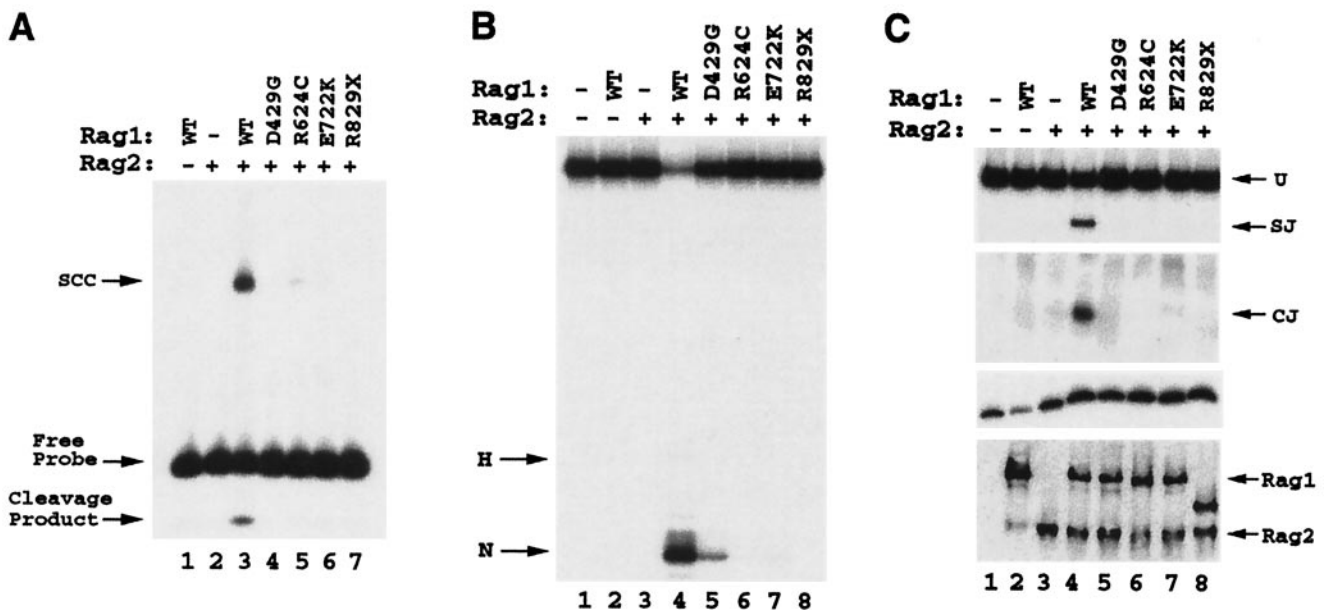


**Fig. 2.** Missense mutations in RAG1 found in OS5, OS9, OS10, and OS11 are not active for 12 RSS binding and cleavage or for rearrangement of episomal recombination substrates. gstRAG1 wild-type (WT), D429G, R624C, E722K, and R829X proteins were incubated with gstRAG2 proteins and  $^{32}P$ -labeled 12 RSS and assayed for stable cleavage complex formation (A), for 12 RSS nicking in the presence of  $Mg^{2+}$  as the divalent cation (B), and for recombination of pJH200 substrate (C). Recombination activity was evaluated by using dilutions in the linear range of the PCR for signal joint (SJ) formation, by using primers RA5 and RA14 for coding joint (CJ) formation and primers OOP2 and CR3 for coding joint formation (30). U represents the unrecombined substrate. RAG1 and RAG2 proteins were detected by using anti-gst antibody from the cell extracts of transfected cells for each recombination assay to permit evaluation of appropriate levels of protein expression.

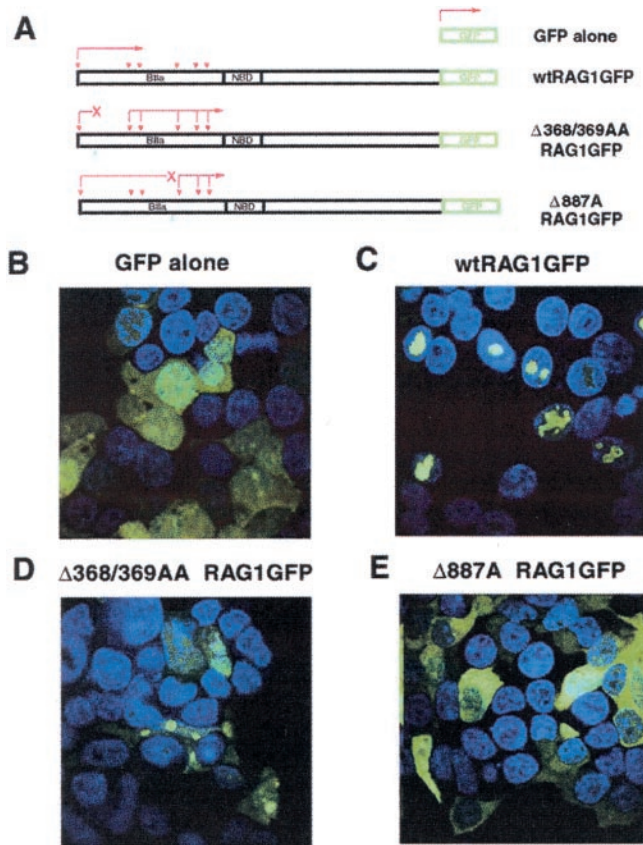


**Fig. 3.** RAG1 protein is generated from alleles  $\Delta 368A/369A$  and  $\Delta 887A$  but is mislocalized. (A) Diagram of wild-type RAG1 and frameshift deletion alleles  $\Delta 368A/369A$  and  $\Delta 887A$  with green fluorescent protein fused in frame to the 3' end. The red triangles mark potential sites of internal initiation downstream between the bona fide ATG and the NBD (nonamer binding domain) that is essential for the activity of the recombinase, and the blue triangles indicate the nucleotide deletions. BIIA indicates a basic motif at the N terminus of RAG1 that is involved in nuclear localization of RAG1 and enhancement of recombination activity. (B, C, and D) Confocal laser scanning microscopy images of 293T cells expressing wtRAG1GFP (B),  $\Delta 368A/369A$  RAG1GFP (C), and  $\Delta 887A$  RAG1GFP (D). Nuclei are stained blue with DAPI.

detect these fusions after transfection in 293T cells (Fig. 3A). Interestingly, fluorescence was observed in cells transfected with all three fusion constructs (Fig. 3C–E). Wild-type RAG1GFP localizes to the nucleus as expected (24), whereas the GFP fusions to  $\Delta 368A/369A$  and  $\Delta 887A$  have aberrant patterns of localization, with the majority of the fluorescence located in the cytoplasm and with only a small portion noted in the nucleus. These findings suggest that the frameshift deletion alleles of RAG1 can indeed produce protein that maintains the proper reading frame of at least the C-terminal region.

To determine whether the proteins produced from  $\Delta 368A/369A$  and  $\Delta 887A$  alleles were full length or truncated, we used pEBB vectors expressing RAG1 alleles with an HA tag fused in frame to the C terminus. RAG1 isolated by using HA-coupled beads from cells metabolically labeled with [ $^{35}$ S]methionine and cysteine revealed that the  $\Delta 368A/369A$  RAG1–3' HA allele generated a protein that was approximately 20 kDa smaller than the precipitated full-length RAG1 protein (Fig. 4B, lanes 2 and 3). Novel products from the  $\Delta 887A$  allele were not readily observed (data not shown). In the adjacent lanes are HA-tagged RAG1 proteins that are initiated from methionines 202 (M2) and 183 (M1), which are

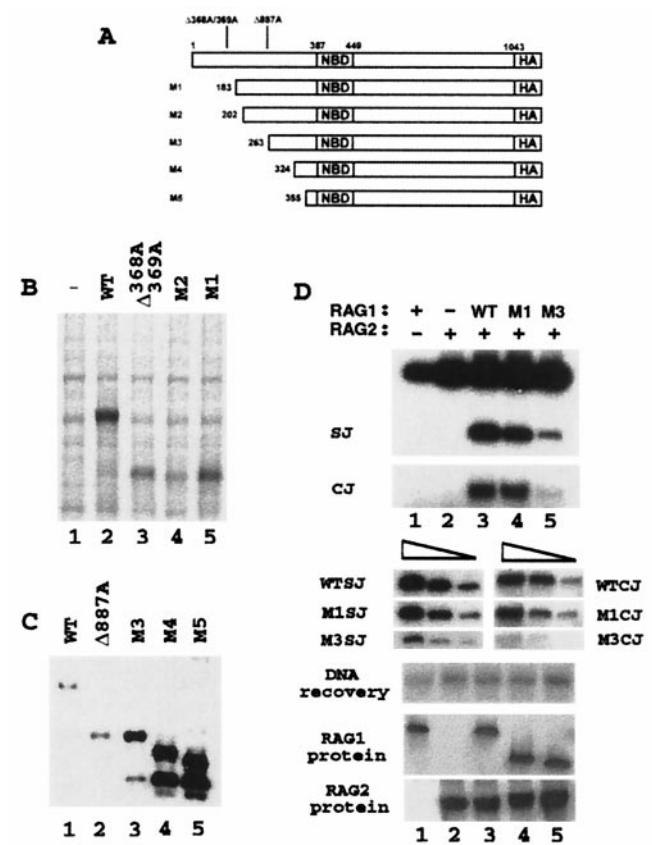


**Fig. 4.** RAG1  $\Delta 368A/369A$  is initiated from methionine 183, and Rag1  $\Delta 887A$  is initiated from methionine 263. (A) Diagram of 3' HA-tagged RAG1 constructs. (B) HA-tagged forms of wild-type (WT) RAG1 (lane 2),  $\Delta 368A/369A$  RAG1 (lane 3), methionine 202 RAG1 (M2; lane 4), and methionine 183 RAG1 (M1; lane 5) were isolated from 293T cells transiently transfected with equal amounts of plasmid and metabolically labeled with [ $^{35}$ S]methionine and cysteine. (C) Western blot analysis using anti-HA antibody 12CA5 to detect 3' HA-tagged RAG1 isoforms coprecipitated with gstrAG2 (amino acids 1–383) after cotransfection in 293T cells. Lanes: 1, wild-type RAG1; 2,  $\Delta 887A$  RAG1; 3, methionine 263 RAG1 (M3); 4, methionine 324 RAG1 (M4); and 5, methionine 355 RAG1 (M5). (D) Recombination assays for full-length RAG1 and the M1 and M3 truncated proteins (the recovered plasmid was used at a 1:50 dilution). Ten micrograms of full-length plasmid was transfected into cells, and 4  $\mu$ g of M1- and M3-expressing pEBB plasmid was used to attain comparable levels of protein expression. Serial dilutions (1:10, 1:40, 1:100) are shown, as well as Western blots demonstrating RAG1 protein expression (detected with RAG1 antibody R1P7, a kind gift from the Schatz lab) and gstrAG2 (amino acids 1–383) protein levels (detected by using an anti-gst antibody).

the second and first methionines found after  $\Delta 368A/369A$  (Fig. 4B, lanes 4 and 5). Comigration of the product from the  $\Delta 368A/369A$  allele with the protein starting from methionine 183 suggests that the RAG1 truncated protein produced from  $\Delta 368A/369A$  is initiated from the first methionine encountered after the two-nucleotide deletion.

The inability to detect a protein from the  $\Delta 887A$  allele suggested that a RAG1 protein initiated from a nonstandard ATG might be unstable when expressed alone. Hence we coexpressed wild-type and  $\Delta 887A$  RAG1–3' HA plus the gstrAG2 active core, affinity purified the complexes by using glutathione beads, and detected the HA-tagged proteins by Western blot analysis. After coexpression with Rag2, we were able to isolate a protein that migrated approximately 30 kDa faster than the full-length RAG1 protein (Fig. 4C, lanes 1 and 2). In the adjacent lanes (lanes 3–5) are HA-tagged RAG1 proteins

initiated from methionines 263, 324, and 355, which reveal that the product from the RAG1  $\Delta$ 887A allele starts from methionine 263.

To compare the inherent recombination capacity of the truncated forms of RAG1 to that of wild-type full-length protein, recombination assays were performed by using RAG1 alleles, where the protein was initiated directly from either methionine 183 (M1) or 263 (M3) (expressed protein diagrammed in Fig. 4A) rather than in the context of a frameshifted full-length allele. Whereas the recombination activity of the M3 protein was only approximately 10% of wild type, the M1 protein demonstrated essentially wild-type levels of activity for recombination of the pJH200 episomal plasmid substrate in transient transfection assays (Fig. 4D). Similar levels of activity were noted on the inversional substrate pJH288 (data not shown). *In vitro* analysis of the activities of the M1 and M3 proteins was prevented by the poor expression levels of *gst* fusions of both proteins (data not shown).

## Discussion

Taken together, the data presented in this study provide a combination of genetic and biochemical evidence to suggest that the RAG1 frameshift deletion alleles isolated from seven patients with Omenn's syndrome are initiated from internal methionines and produce RAG1 truncations that retain sufficient activity to generate a partial recombination phenotype. Interestingly, the  $\Delta$ 368A/369A deletion accounts for the majority of mutant genes in our series of unrelated probands. Although we cannot exclude the possibility that the 368/369 nucleotides represent a hot spot for mutations, the fact that these alleles were found mainly in patients from Yugoslavia and in the remaining case from Italy, which is a bordering country, is consistent with a founder effect.

Previous studies had demonstrated that forms of mouse and human RAG1 lacking the N terminus (amino acids 1–383) could effectively perform a broad array of DNA recognition and cleavage functions as assessed *in vitro* (9, 34) and could in addition mediate recombination of both episomal plasmid substrates and of endogenous antigen receptor loci (20, 21, 35). However, the importance of the RAG1 N terminus for enhancing the efficiency of the recombination reaction, particularly of endogenous loci, has also been highlighted (20, 21). The subset of Omenn's patients with antigen receptor repertoires of limited clonality described in this study provide genetic evidence consistent with the model that the RAG1 N terminus is dispensable for limited recombinase activity, but that efficient recombination requires an intact N terminus.

In determining the exact mechanistic reasons for the reduced recombination products generated by either of the frameshift deletion alleles, a number of factors can be considered. First, in the transient transfection assays and in the lymphocytes of patients, the efficiency of translation of the internally initiated proteins is likely less than that of wild-type RAG1 because methionines 183 and 263 are located in the context of suboptimal Kozak consensus sequences (36) and are not the first methionines encountered by the translation machinery. Second, as indicated by the localization of GFP fusions, the truncations are partly mislocalized because of deletion of portions of the N terminus. In the case of  $\Delta$ 887A, initiation from methionine 263 would delete the BIIA motif (amino acids 219–224) that participates in the interaction with the nuclear localization factor Srp-1. Initiation from methionine 183 of the  $\Delta$ 368A/369A allele would leave the BIIA motif intact, but the lack of amino acids 1–183 could conceivably have global consequences on the N terminus that could adversely affect nuclear localization. It is possible that in both cases the C-terminal interaction with Rch1 or RAG2 might compensate in part, allowing limited transport into the nucleus (24). Third, regions implicated in the enhance-

ment of V(D)J recombination efficiency such as C1, C2, and C3 are deleted in both methionine 183 and 263 truncations and BIIA (20), and C4 is also deleted in the RAG1 263 truncation (21).

In light of these three possibilities, it is interesting that a RAG1 allele directly initiating translation from methionine 263 (M3), which is expressed at levels comparable to that in wild-type protein, is also highly deficient for recombination of episomal plasmids (Fig. 4D). Hence diminished V(D)J recombination in patient OS13 can clearly be pinned to a defect in the function of the protein and not just to diminished protein levels, which may, however, serve to compound the effect. On the other hand, a RAG1 allele directly initiating translation from methionine 183 (M1) appears to recombine plasmid substrates as well as full-length wild-type protein when expressed at comparable levels. Hence the more likely causes of the deficiency observed in patient OS8, for instance, who is homozygous for the frameshift  $\Delta$ 368/369 allele are either (i) inefficient recombination of endogenous antigen receptor loci as opposed to plasmid substrates or (ii) reduced expression of the protein in the context of the frameshift full-length allele. In fact, reduced translation efficiency of RAG1 from the  $\Delta$ 368/369 allele is suggested by the 4-fold reduced recovery of the truncated protein after transient transfection (Fig. 4B; compare lanes 2 and 3).

Translation initiation from alternative start sites has been documented for the von Hippel–Landau protein (pVHL), where a biologically active isoform spanning amino acids 54–213 is generated (37). In addition, N-terminally truncated isoforms of the Egr3 protein implicated in regulating gene expression underlying neuronal plasticity have been identified and demonstrate differential transcriptional activation properties (38). Initiation of protein translation from internal methionines to generate partially active protein isoforms has also been suggested as the basis of variants of typically severe clinical syndromes. The partially active truncated proteins lead to milder phenotypes with slower rates of progression. In cases of Becker muscular dystrophy (39, 40), a milder variant of Duchenne's muscular dystrophy, the production of N-terminally truncated isoforms is predicted to result after frameshift deletions. In Fanconi's anemia (41) amino-terminal truncated forms of Fanconi's anemia complementation group C protein have been detected from cell lines of individuals affected with milder forms of the disease. The identification of a similar mechanism of internal methionine usage in RAG1 as a cause of Omenn's syndrome supplies another example of a biochemically less severe phenotype likely resulting from the generation of amino-terminal truncated proteins. It is interesting to consider that this type of compensatory mechanism may underlie other clinically variable syndromes.

S.S. thanks Stuart Aaronson for his kind guidance and support and Z.-Q. Pan for guidance and critical review of the manuscript. We thank M. Mirolo for technical assistance. This work was funded by Telethon Grant E0917 to A.V., by a National Institutes of Health (NIH) Predoctoral Training Grant in Cancer to S.S., by NIH Grant AI40191 and a Cancer Research Institute Investigator Award to Zhen-Qiang Pan, and by NIH Grant AI45996-02 and a Cancer Research Institute Investigator Award to P.C. S.S. is currently supported by NIH Postdoctoral Training Grant DK07757, awarded to the Division of Nephrology, Department of Medicine, Mount Sinai School of Medicine. Confocal laser scanning microscopy was performed at the Mount Sinai School of Medicine–Confocal Laser Scanning Microscopy core facility with Scott Henderson, supported with funding from NIH Shared Instrumentation Grant 1 S10 RR0 9145-01 and National Science Foundation Major Research Instrumentation Grant DBI-9724504. A.V. is the recipient of a travel fellowship for international scientific exchange from the Associazione Italiana per la Ricerca sul Cancro (Italy). This is manuscript 43 of the Cariplo–ITBA project Genoma 2000 directed by R. Dulbecco and funded by Cariplo.

1. Fischer, A. & Malissen, B. (1998) *Science* **280**, 237–243.
2. Schwarz, K., Gauss, G. H., Ludwig, L., Pannicke, U., Li, Z., Lindner, D., Friedrich, W., Seger, R. A., Hansen-Hagge, T. E., Desiderio, S., Lieber, M. R. & Bartram, C. R. (1996) *Science* **274**, 97–99.
3. Villa, A., Santagata, S., Bozzi, F., Giliani, S., Frattini, A., Imberti, L., Gatta, L. B., Ochs, H. D., Schwarz, K., Notarangelo, L. D., Vezzoni, P. & Spanopoulou, E. (1998) *Cell* **93**, 885–896.
4. Villa, A., Santagata, S., Bozzi, F., Imberti, L. & Notarangelo, L. D. (1999) *J. Clin. Immunol.* **19**, 87–97.
5. Tonegawa, S. (1983) *Nature (London)* **302**, 575–581.
6. Steen, S. B., Gomelsky, L. & Roth, D. B. (1996) *Genes Cells* **1**, 543–553.
7. Eastman, Q. M., Leu, T. M. & Schatz, D. G. (1996) *Nature (London)* **380**, 85–88.
8. Hiom, K. & Gellert, M. (1997) *Cell* **88**, 65–72.
9. van Gent, D. C., McBlane, J. F., Ramsden, D. A., Sadofsky, M. J., Hesse, J. E. & Gellert, M. (1995) *Cell* **81**, 925–934.
10. McBlane, J. F., van Gent, D. C., Ramsden, D. A., Romeo, C., Cuomo, C. A., Gellert, M. & Oettinger, M. A. (1995) *Cell* **83**, 387–395.
11. Besmer, E., Mansilla-Soto, J., Cassard, S., Sawchuk, D. J., Brown, G., Sadofsky, M., Lewis, S. M., Nussenzweig, M. C. & Cortes, P. (1998) *Mol. Cell* **2**, 817–828.
12. Shockett, P. E. & Schatz, D. G. (1999) *Mol. Cell Biol.* **19**, 4159–4166.
13. Santagata, S., Besmer, E., Villa, A., Bozzi, F., Allingham, J. S., Sobacchi, C., Haniford, D. B., Vezzoni, P., Nussenzweig, M. C., Pan, Z. Q. & Cortes, P. (1999) *Mol. Cell* **4**, 935–947.
14. Callebaut, I. & Mornon, J. P. (1998) *Cell Mol. Life Sci.* **54**, 880–891.
15. Spanopoulou, E., Zaitseva, F., Wang, F. H., Santagata, S., Baltimore, D. & Panayotou, G. (1996) *Cell* **87**, 263–276.
16. Difilippantonio, M. J., McMahan, C. J., Eastman, Q. M., Spanopoulou, E. & Schatz, D. G. (1996) *Cell* **87**, 253–262.
17. Landree, M. A., Wibbenmeyer, J. A. & Roth, D. B. (1999) *Genes Dev.* **13**, 3059–3069.
18. Kim, D. R., Dai, Y., Mundy, C. L., Yang, W. & Oettinger, M. A. (1999) *Genes Dev.* **13**, 3070–3080.
19. Fugmann, S. D., Villey, I. J., Ptaszek, L. M. & Schatz, D. G. (2000) *Mol. Cell* **5**, 97–107.
20. Roman, C. A., Cherry, S. R. & Baltimore, D. (1997) *Immunity* **7**, 13–24.
21. McMahan, C. J., Difilippantonio, M. J., Rao, N., Spanopoulou, E. & Schatz, D. G. (1997) *Mol. Cell Biol.* **17**, 4544–4552.
22. Rodgers, K. K., Bu, Z., Fleming, K. G., Schatz, D. G., Engelman, D. M. & Coleman, J. E. (1996) *J. Mol. Biol.* **260**, 70–84.
23. Cortes, P., Ye, Z. S. & Baltimore, D. (1994) *Proc. Natl. Acad. Sci. USA* **91**, 7633–7637.
24. Spanopoulou, E., Cortes, P., Shih, C., Huang, C. M., Silver, D. P., Svec, P. & Baltimore, D. (1995) *Immunity* **3**, 715–726.
25. Mizushima, S. & Nagata, S. (1990) *Nucleic Acids Res.* **18**, 5322.
26. Santagata, S., Bhattacharyya, D., Wang, F. H., Singha, N., Hodtsev, A. & Spanopoulou, E. (1999) *J. Biol. Chem.* **274**, 16311–16319.
27. Santagata, S., Aidinis, V. & Spanopoulou, E. (1998) *J. Biol. Chem.* **273**, 16325–16331.
28. Hesse, J. E., Lieber, M. R., Gellert, M. & Mizuuchi, K. (1987) *Cell* **49**, 775–783.
29. Aidinis, V., Bonaldi, T., Beltrame, M., Santagata, S., Bianchi, M. E. & Spanopoulou, E. (1999) *Mol. Cell Biol.* **19**, 6532–6542.
30. Roman, C. A. & Baltimore, D. (1996) *Proc. Natl. Acad. Sci. USA* **93**, 2333–2338.
31. Wu, K., Fuchs, S. Y., Chen, A., Tan, P., Gomez, C., Ronai, Z. & Pan, Z. Q. (2000) *Mol. Cell Biol.* **20**, 1382–1393.
32. Alam, S. L., Atkins, J. F. & Gesteland, R. F. (1999) *Proc. Natl. Acad. Sci. USA* **96**, 14177–14179.
33. Wilson, G. M. & Brewer, G. (1999) *Genome Res.* **9**, 393–394.
34. Sawchuk, D. J., Weis-Garcia, F., Malik, S., Besmer, E., Bustin, M., Nussenzweig, M. C. & Cortes, P. (1997) *J. Exp. Med.* **185**, 2025–2032.
35. Sadofsky, M. J., Hesse, J. E., McBlane, J. F. & Gellert, M. (1994) *Nucleic Acids Res.* **22**, 550.
36. Kozak, M. (1984) *Nucleic Acids Res.* **12**, 857–872.
37. Iliopoulos, O., Ohh, M. & Kaelin, W. G., Jr. (1998) *Proc. Natl. Acad. Sci. USA* **95**, 11661–11666.
38. O'Donovan, K. J. & Baraban, J. M. (1999) *Mol. Cell Biol.* **19**, 4711–4718.
39. Monaco, A. P., Bertelson, C. J., Liechti-Gallati, S., Moser, H. & Kunkel, L. M. (1988) *Genomics* **2**, 90–95.
40. Malhotra, S. B., Hart, K. A., Klamut, H. J., Thomas, N. S., Bodrug, S. E., Burghes, A. H., Bobrow, M., Harper, P. S., Thompson, M. W., Ray, P. N., *et al.* (1988) *Science* **242**, 755–759.
41. Yamashita, T., Wu, N., Kupfer, G., Corless, C., Joenje, H., Grompe, M. & D'Andrea, A. D. (1996) *Blood* **87**, 4424–4432.